ASIAN JOURNAL OF CIVIL ENGINEERING (BHRC) VOL. 15, NO. 2 (2014)
PAGES 179-212

ENHANCED BAT ALGORITHM FOR OPTIMAL DESIGN OF SKELETAL STRUCTURES

A. Kaveh* and P. Zakian
Department of Civil Engineering, Iran University of Science and Technology, Narmak, Tehran-16, Iran.

Received: 10 June 2013; **Accepted:** 2 September 2013

ABSTRACT

In this article, an improvement is proposed for bat algorithm and it is utilized for size optimization of skeletal structures consisting of truss and frame structures. Various optimization problems are implemented to demonstrate the ability of the enhanced bat algorithm. These numerical examples are along with different constraints and loading conditions such as stress, displacement and frequency constraints, static and time history dynamic loadings. Furthermore, these optimization problems are in two form of discrete and continuous. Results show the suitability and efficiency of the present algorithm for optimal design of skeletal structures.

Keywords: Structural optimization; an enhanced bat algorithm; truss structures; frame structures; continuous and discrete optimization.

1. INTRODUCTION

Optimal design of structures aims to design a structure with minimum weight, or minimize an objective function value corresponding to minimal cost of the structure, while the corresponding design criteria are satisfied.

Different classifications exist for structural design optimization. Based on the variable types to be optimized, three kind of optimization are considered as: size optimization, shape (geometry) optimization and topology optimization. Optimization algorithms can be generally categorized as deterministic and non-deterministic (random) algorithms. Meta-heuristics are well-known non-deterministic optimization algorithms that are utilized in engineering optimization problems and are in a progressive state of development. Many researchers are concerned with structural design optimization via various meta-heuristic

* E-mail address of the corresponding author: alikaveh@iust.ac.ir (A. Kaveh)

algorithms. Here, only a few of these are summarized:

Camp [1] optimized the space trusses using Big Bang–Big Crunch (BB-BC) which is a kind of meta-heuristic algorithm, Gomes [2] employed the particle swarm optimization (PSO) algorithm for size and geometry optimization of truss structures, Li et al. [3] used a heuristic particle swarm optimizer for optimization of pin connected structures, Design optimization of 3D steel structures with comparison of genetic algorithms versus classical techniques was performed by Prendes Gero et al. [4], Salajegheh & Heidari [5] utilized wavelets, neural network and genetic algorithm (GA) for optimum design of structures under earthquake loading, Liu, et al. [6] performed seismic design optimization of steel frame buildings based on life cycle cost considerations, Kaveh & Talatahari [7] presented an improved ant colony optimization (IACO) for the design of planar steel frames. Kaveh & Talatahari [8, 9] developed the charged system search algorithm and applied to optimal design of skeletal structures. Kaveh & Farhoudi developed Dolphine optimization [10], and Kaveh & Khayatazad [11] proposed Ray optimization for truss and frame optimization. Golizadeh & Salajegheh [12] employed a meta-modeling based real valued PSO algorithm for optimizing structures subjected to time history loading, Kaveh & Zakian [13] performed optimal seismic design of special reinforced concrete shear walls via charged system search algorithm by defining several constraints and generating shear wall section database so as to have a discrete optimization.. Kaveh & Zakian [14] accomplished optimal design of steel moment and shear frames under seismic loading using charged system search and improved harmony search algorithms considering drift and stress constraints via simultaneous static-dynamic structural analysis.

This paper presents an improvement on bat algorithm to carry out size optimization of skeletal structures consisting of trusses and frames. Various optimization problems are implemented to demonstrate the ability of the present enhanced bat algorithm. These design examples are associated with different constraints and loadings such as stress, displacement and frequency constraints, static and time history dynamic loadings. Here, both discrete and continuous optimization problems are studied. Results indicate the efficiency of the algorithm for design optimization of skeletal structures.

2. BAT ALGORITHM

2.1 Definitions

Bat algorithm (BA) is a meta-heuristic optimization algorithm which was presented by Yang [15]. This algorithm is inspired from the echolocation behavior of microbats. In echolocation behavior, each pulse only lasts a few thousandths of a second (up to about 8–10 *ms*). Nevertheless, it has a constant frequency which is usually in the range of 25–150 *kHz* corresponding to the wavelengths of 2–14 *mm*. In BA, the echolocation properties of microbats can be idealized as the following rules [16]:

1. All bats use echolocation to sense distance, and they also ‘‘know’’ the difference between food/prey and background barriers.

2. Bats randomly move with a velocity of v_i at position x_i with a fixed frequency f, varying wavelength λ, and loudness A_0 to search for prey. They can automatically tune the

wavelength (or frequency) of their emitted pulses and tune the rate of pulse emission $r \in [0,1]$, depending on the proximity of their target,

3. Although the loudness can vary in different ways, it is supposed that the loudness varies from a large (positive) A_0 to a minimum constant value A_{min}.

For each bat (i), its position x_i and velocity v_i in a *nv*-dimensional search space should be defined. x_i and v_i should be subsequently updated during the iterations. Adjusting frequency and the new solutions x_i^t and velocities v_i^t at time step *t* can be calculated by:

$$f_i = f_{\min} + \beta(f_{\max} - f_{\min}) \quad (1)$$

$$v_i^t = v_i^{t-1} + f_i(x_i^{t-1} - x_{cgbest}) \quad (2)$$

$$x_i^t = x_i^{t-1} + v_i^t \quad (3)$$

where β in the range of [0,1] is a random vector drawn from a uniform distribution. Here, x_{cgbest} is the current global best location (solution), which is located after comparing all the solutions among all the n bats. As the product $\lambda_i f_i$ is the velocity increment, either f_i (or λ_i) can be used to adjust the velocity change while fixing the other factor λ_i (or f_i), depending on the type of the problem of interest. For implementation, $f_{\min} = 0$ and $f_{\max} = 100$ are used, depending on the domain size of the problem of interest. Initially, each bat is randomly assigned a frequency that is drawn uniformly from $[f_{\min}, f_{\max}]$. For the local search part, once a solution is selected among the current best solutions, a new solution for each bat is generated locally using a local random walk:

$$x_{new} = x_{old} + \varepsilon \prec A_i^t \succ \quad (4)$$

where the random number ε is drawn from $[-1,1]$, while $\prec A_i^t \succ$ is the average loudness of all the bats at this time step. The update of the velocities and positions of bats have some similarities to the procedure in the standard particle swarm optimization as f_i essentially controls the pace and range of the movement of the swarming particles. To a degree, BA can be considered as a balanced combination of the standard particle swarm optimization and the intensive local search controlled by the loudness and pulse rate. Once a bat found its prey, the loudness usually decreases and the rate of pulse emission increases. In this case, the loudness can be chosen as any value of convenience. For simplicity, $A_0 = 1$ and $A_{min} = 0$ can be used. Assuming $A_{min} = 0$ means that a bat has just found the prey and temporarily stop emitting any sound, we have:

$$A_i^{t+1} = \alpha A_i^t \quad (5)$$

$$r_i^{t+1} = r_i^0[1 - \exp(-\gamma t)] \quad (6)$$

In which α and γ are constants. In fact, α is similar to the cooling factor of a cooling

schedule in the simulated annealing. For any $\alpha > 0$ *and* $\gamma < 1$:

$$\lim_{t\to\infty}[A_i^{t+1}] = 0, \qquad \lim_{t\to\infty}[r_i^{t+1}] = r_i^0 \tag{7}$$

In the simplest case, $\alpha = \gamma$ can be used. It is worth pointing that the bat algorithm is not just another metaheuristic. Compared with existing metaheuristics, it has two advantages: frequency tuning and dynamic control of exploration and exploitation by automatic switching to intensive exploitation if necessary. It uses the frequency-based tuning and pulse emission rate changes to mimic bat behavior, which leads to good convergence and simpler implementation compared with other algorithms. In addition, the balance of exploration and exploitation is important; a simple fixed ratio of exploration to exploitation is not necessarily a good strategy.

Bat algorithm uses a dynamic strategy for exploration and exploitation. Like the autohoming of bats on their prey, the variations in pulse emission rates and loudness essentially control how exploration and exploitation are used. In fact, auto switching from exploration to more extensive exploitation can be achieved when the optimality is approaching; thus, the algorithm can be very efficient in applications. Pseudo code of the bat algorithm has been illustrated in Fig.1.

Objective function Obj(X) , $X=[x_1,x_2,\ldots,x_{nv}]^T$
Begin
Initialize the bat population x_i and v_i (i=1,2,..,n)
Define pulse frequency of f_i at x_i
Initialize pulse rates r_i and the loudness A_i
While (t<maximum number of iterations)
Generate new solutions by adjusting frequency and update velocities and positions (equation 1, 2 and 3)
If (rand >r_i)
Select a solution among the best solutions randomly;
Generate a local solution around the selected best solution by a local random walk (equation 4)
End if
If (rand<A_i and $f(x_i)<f(x^{cgbest})$)
Accept the new solution
Increases r_i and decrease a_i
End if
Rank the bats at each iteration and store their current global best x^{cgbest}
End while
Post processing the results
End

Figure 1. Pseudo code of bat algorithm for optimization.

2.2 Improvement

Exploration ability of the bat algorithm is favorable. But, it needs high number of iteration to lead to a desirable solution. Here, with defining dynamic θ scale factor parameter (a factor that limits the step sizes of random walks for local search), an improvement is proposed for this algorithm. Proper tuning of this parameter reduces the number of the iterations (hence the computational time). In addition, this improvement can provide easy adjustment of the

bat algorithm for discrete optimization problems. Dynamic scale factor θ parameter may be formulated as:

$$\theta(iter) = \theta_{\max} \exp((\frac{Ln(\frac{\theta_{\min}}{\theta_{\max}})}{\theta_{\max}}) \cdot iter) \tag{8}$$

This formulation is inspired from [17]. They proposed this relationship for bandwidth parameter of harmony search algorithm.

Instead of using Eq. (4), for improved version the following equation can be used:

$$x_{new} = x_{old} + \varepsilon.\theta(iter) \tag{9}$$

where *iter* stands for current iteration. For solving design examples, this enhanced version is used. In continuous optimization problems, $\theta_{\max}$ and $\theta_{\min}$ should be taken such as 1 and 0.001, respectively whereas in discrete optimization problems, these should be taken such as 10 and 0.1, respectively. However, these values are commonly recommended for tuning parameters of optimization problems and for many problems these need to be well-adjusted as these parameters are highly problem dependent.

3. STATEMENT OF THE DESIGN OPTIMIZATION PROBLEM

Since in size optimization usually design variables are in the form of thickness or dimensions of the members of the structure, size optimization of skeletal structures involves reaching at optimum values for cross-sectional areas of structural members that minimize the structural weight *W*. This minimal design also has to satisfy inequality or equality constraints that restrict design variable sizes and structural responses. Hence, the optimal structural design problem may be expressed as:

$$\begin{aligned} &Minimize && W(X) \\ &subject\ to && g_j(X) \le 0 \\ &X = [x_1, x_2, x_3, ..., x_n]^T \\ &i = 1,2,3,...,nv \\ &x_i \in R^d \end{aligned} \tag{10}$$

$$Minimize \qquad Obj(X) = W(X) \times f_{penalty}(X) \tag{11}$$

Where X is the vector of design variables containing the cross section areas, *nv* is the number of design variables or the number of member groups, and R^d is the domain of the design variables. Here, *Obj*(X) is the objective function or penalized weight of the structure,

W(X) is the structural weight function, and $f_{\text{penalty}}(X)$ is penalty function in order to control the constraints:

$$W(X) = \sum_{i=1}^{nv} \gamma_i \cdot x_i \cdot l_i \tag{12}$$

$$f_{penalty}(X) = (1 + \kappa_1 \cdot \nu)^{\kappa_2} \ , \ \nu = \sum_{i=1}^{n} \max[0, \nu_i] \tag{13}$$

Where l_i is the length, and γ_i is the material density of the member *i*. Here, the parameters κ_1 and κ_2 for the penalty function are selected as [14]. ν represents the sum of the violated constraints.

4. NUMERICAL EXAMPLES

Seven design examples are chosen and solved by the present algorithm in order to demonstrate the efficiency of the natural inspired bat algorithm. These optimization examples are along with different constraints and analyses. In Examples 1 and 2, benchmark truss structures are optimized, static structural analysis is performed for checking stress and displacement constraints, and type of the problems are continuous. In Examples 3 and 4, two benchmark truss structures is optimized, eigenvalue analysis is performed for checking frequency constraints and type of these problems is continuous too. In Examples 5, a benchmark moment resisting frame structure is optimized, static analysis is performed for checking displacement constraint and type of this problem is discrete. Design variables are selected from W-section database of AISC. In Example 6, a benchmark moment resisting frame structure is optimized, time history dynamic analysis is performed for checking drift constraint and type of this problem is discrete as well. Design variables are selected from an available section database.

In Example 7, a truss tower structure is optimized, static and time history dynamic analysis is performed for checking drift and stress constraints and type of this problem is continuous.

For the following Examples 1, 2, 4, and 5, the number of bats is taken as 40, and 500 iterations are selected for optimization procedures. Therefore, about 20,000 structural analyses are carried out for each example.

For Example 3, 40 bats are considered, and 500 iterations are used. Hence 25,000 structural analyses are performed.

For Examples 6 and 7, 30 bats - 200 iterations and 35 bats - 200 iterations are selected, respectively. Thus, to complete the optimization procedures about 6000 to 7000 structural analyses are performed, respectively. The α and γ are selected near to 1 and 0.5, respectively. By the proposed improvement, the θ parameter can be tuned in such a way that the algorithm is adjusted easily for discrete variable optimization problems.

Examples 6 and 7, require a large computational time. For these examples convergence curves of four best runs are plotted.

4.1 A 25-bar spatial truss

The geometry and nodal numbers of a 25-bar spatial truss structure are shown in Fig.2. In this example, designs for a multiple load case are performed and the results are compared to those of other optimization techniques employed by researchers. In these studies, the material density is considered as 0.1 lb/in^3 (2767.990 kg/m^3) and the modulus of elasticity is taken as 10,000 *ksi* (68,950 *MPa*). Twenty five members are categorized into eight groups, as follows: (1) A_1, (2) A_2-A_5, (3) A_6-A_9, (4) A_{10}-A_{11}, (5) A_{12}-A_{13}, (6) A_{14}-A_{17}, (7) A_{18}-A_{21}, and (8) A_{22}-A_{25}. Maximum displacement limitations of ± 0.35 *in* (8.89 *mm*) are imposed on every node in all three directions and the axial stress constraints vary for each group as shown in Table 1.The range of cross-sectional areas varies from 0.01 to 3.4 in^2 (0.6452–21.94 cm^2). This spatial truss is subjected to two loading conditions shown in Table 2.

The bat algorithm achieves the best solution near to HBB–BC solution. However, convergence curve of the average of ten independent optimization runs and the best convergence history curve are plotted in Fig 3.Which shows the stability of the algorithm for a certain parameter tuning. Table 3 presents a comparison of the performance of the BA method and other heuristic algorithms. Here, the result is not the best one among other results but it is comparatively good outcome. θ_{max} and θ_{min} are taken as 1 and 0.0001, respectively. Constraint violation information is shown in Fig.4 Fig.5 for stress and displacement constraints of each load case, respectively.

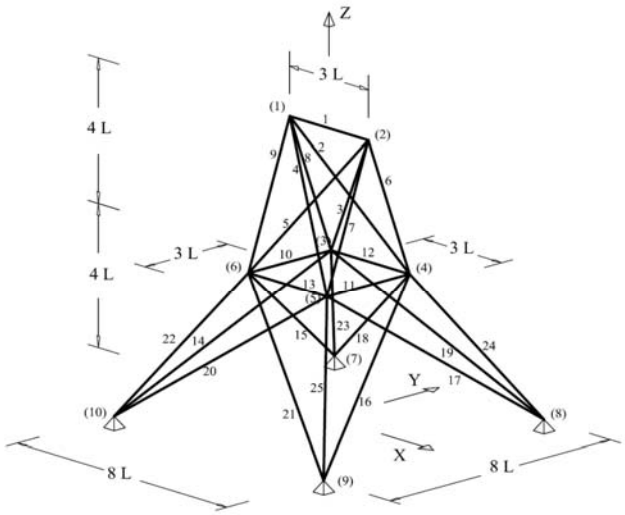

L = 25 in (63.5 cm)

Figure 2. A 25-bar spatial truss

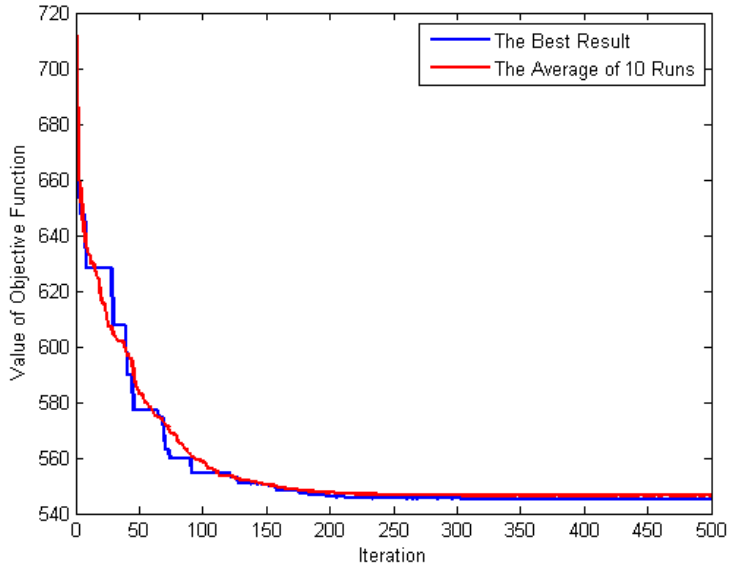

Figure 3. The convergence history for the 25-bar spatial truss obtained by the BA.

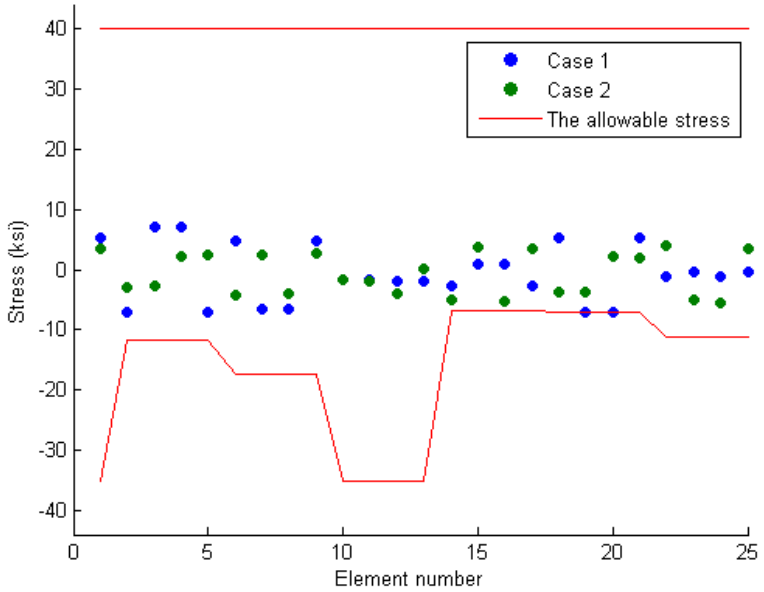

Figure 4. The stress constraints violation details for the optimum 25-bar spatial truss obtained by the BA

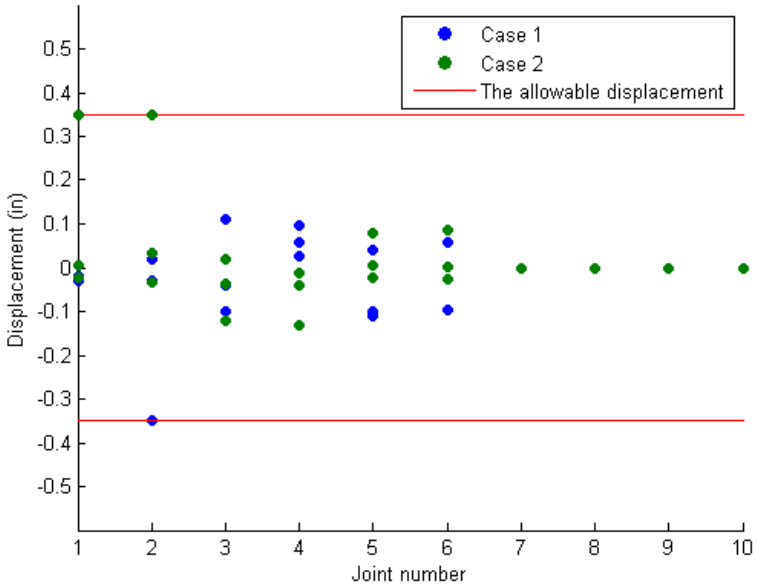

Figure 5. The displacement constraints violation details for the optimum 25-bar spatial truss obtained by the BA.

Table 1: Allowable stress values for the spatial 25-bar truss.

Element group		Compressive stress limitations ksi (MPa)	Tensile stress limitations ksi (MPa)
1	A1	35.092 (241.96)	40.0 (275.8)
2	A_2–A_5	11.590 (79.913)	40.0 (275.8)
3	A_6–A_9	17.305 (119.31)	40.0 (275.8)
4	A_{10}–A_{11}	35.092 (241.96)	40.0 (275.8)
5	A_{12}–A_{13}	35.092 (241.96)	40.0 (275.8)
6	A_{14}–A_{17}	6.759 (46.603)	40.0 (275.8)
7	A_{18}–A_{21}	6.959 (47.982)	40.0 (275.8)
8	A_{22}–A_{25}	11.082 (76.41)	40.0 (275.8)

Table 2: Loading details for the spatial 25-bar truss.

Node	Case 1			Case 2		
	P_x	P_y	P_z	P_x	P_y	P_z
	kips (kN)			kips (kN)		
1	0	20(89)	-5(22.25)	1(4.45)	10(44.5)	-5(22.25)
2	0	-20(89)	-5(22.25)	0	10(44.5)	-5(22.25)
3	0	0	0	0.5(2.22)	0	0
6	0	0	0	0.5(2.22)	0	0

Table 3: Optimal design comparison for the spatial 25-bar truss.

Element group		Optimal cross-sectional areas (in^2)												
		Lee & Geem [26]	Li et al.[3]			Camp [1]	Lamberti [27]	Lamberti & Pappalettee [28]	Kaveh & Talatahari [29]	Kaveh & Talatahari [30]	Degertekin [31]		Present study	
		HS	PSO	PSOPC	HPSO	BB–BC	CMLPSA	IHS	HPSACO	HBB–BC	EHS	SAHS	(in^2)	(cm^2)
1	A_1	0.047	9.863	0.010	0.010	0.010	0.0100	0.0100	0.010	2.6622	0.010	0.010	0.01000	0.064516
2	A_2-A_5	2.022	1.798	1.979	1.970	2.092	1.9870	1.9871	2.054	1.9930	1.995	2.074	1.97889	12.76701
3	A_6-A_9	2.950	3.654	3.011	3.016	2.964	2.9935	2.9935	3.008	3.0560	2.980	2.961	3.00472	19.38525
4	A_{10}-A_{11}	0.010	0.100	0.100	0.010	0.010	0.0100	0.0100	0.010	0.0100	0.010	0.010	0.01000	0.064516
5	A_{12}-A_{13}	0.014	0.100	0.100	0.010	0.010	0.0100	0.0100	0.010	0.0100	0.010	0.010	0.01000	0.064516
6	A_{14}-A_{17}	0.688	0.596	0.657	0.694	0.689	0.6894	0.6839	0.679	0.6650	0.696	0.691	0.68880	4.443862
7	A_{18}-A_{21}	1.657	1.659	1.678	1.681	1.601	1.6769	1.6769	1.611	1.6420	1.679	1.617	1.67834	10.82798
8	A_{22}-A_{25}	2.663	2.612	2.693	2.643	2.686	2.6621	2.6622	2.678	2.6790	2.652	2.674	2.65270	17.11416
Weight(lb)		544.38	627.08	545.27	545.19	545.38	545.15	545.15	544.99	545.16	545.49	545.12	545.16879	2425.03160 (N)
Average weight (lb)		N/A	N/A	N/A	N/A	545.78	N/A	N/A	545.52	545.66	546.52	545.94	546.44644	
Number of structural analyses		15,000	150,000	150,000	125,000	20,566	400	1050	9875	12,500	10,391	9051	20,000	

4.2 A 72-bar spatial truss

The second test case is the spatial 72-bar truss shown in Fig.6. The elastic modulus of the material is 10,000 ksi (68,950 MPa) while density is 0.1 lb/in^3 (2767.990 kg/m^3). The cross-sectional areas members are included as design variables and are divided into 16 groups: (1) A_1–A_4, (2) A_5–A_{12}, (3) A_{13}–A_{16}, (4) A_{17}–A_{18}, (5) A_{19}–A_{22}, (6) A_{23}–A_{30}, (7) A_{31}–A_{34}, (8) A_{35}–A_{36}, (9) A_{37}–A_{40},(10) A_{41}–A_{48}, (11) A_{49}–A_{52}, (12) A_{53}–A_{54}, (13) A_{55}–A_{58}, (14) A_{59}–A_{66},(15) A_{67}–A_{70}, (16) A_{71}–A_{72}.The allowable stress for all members is 25 ksi (172.375 MPa) (the same in tension and compression) and the displacement of top nodes must be less than 0.25 in (0.635 cm) in both the x and y directions. For the 72-bar the minimum permitted

cross-sectional area of each member is 0.10 in^2 (0.6452 cm^2), and the maximum cross-sectional area of each member is 4.00 in^2 (25.81 cm^2). Table 4 lists the values and directions of the two load cases applied to the 72- bar spatial truss.

Convergence history of the average of ten independent optimization runs and the best run are plotted in Fig.7.The best weight of the BA optimization is 380.05819 lb, while it is the best results after HBB–BC and BB-BC methods, results of some other methods are provided in Table 5. Here, θ_{max} and θ_{min} are taken as 1 and 0.001, respectively. Constraint violation details are plotted in Fig.8 and Fig.9 for stress and displacement subjected to two load cases, respectively.

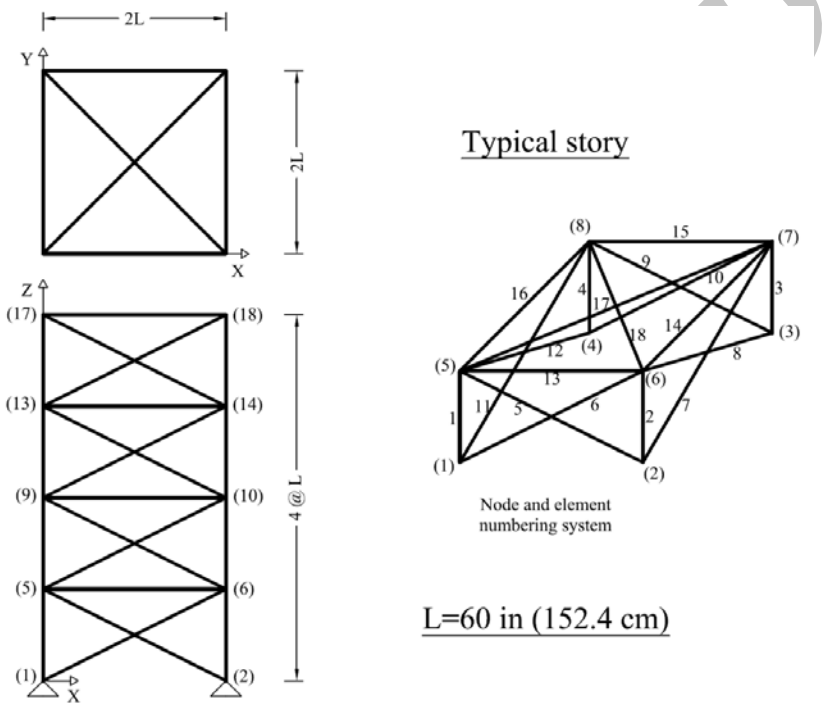

Figure 6. A seventy two-bar spatial truss.

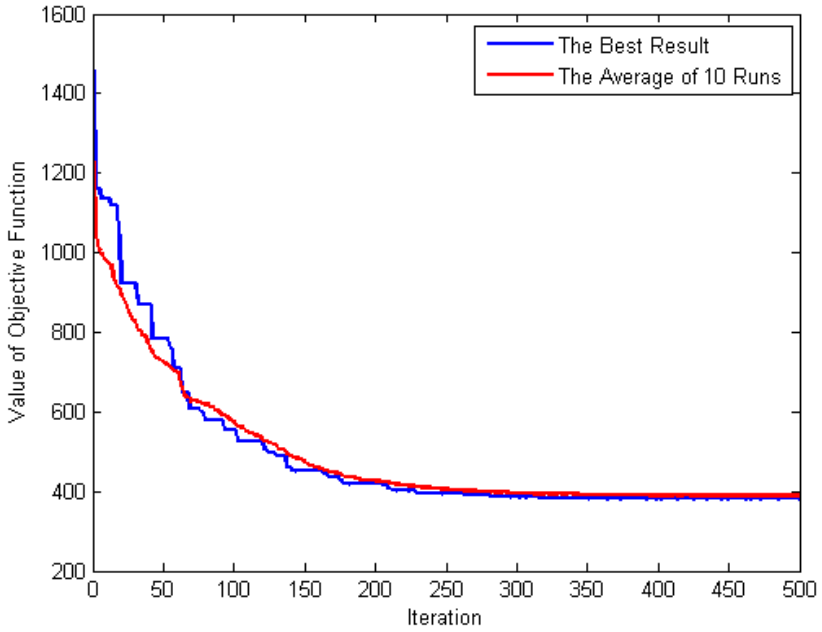

Figure 7. The convergence history for the seventy two-bar spatial truss obtained by the BA.

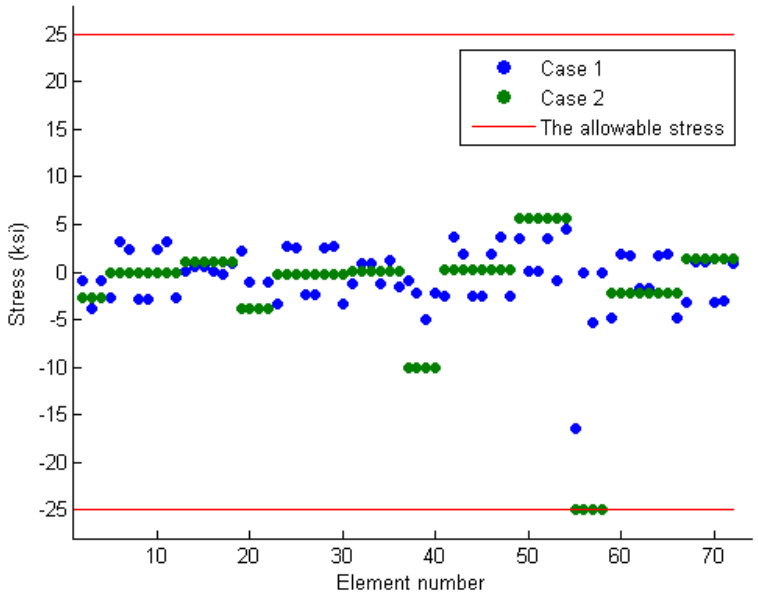

Figure 8. The stress constraints violation details for the optimum seventy two-bar spatial truss obtained by the BA.

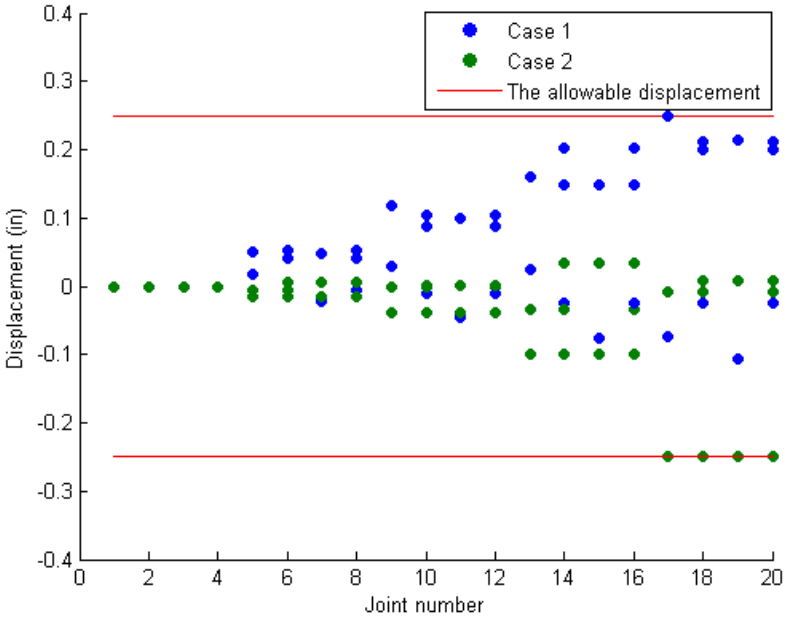

Figure 9. The displacement constraints violation details for the optimum seventy two-bar spatial truss obtained by the BA.

Table 4: Loading details for the seventy two-bar spatial truss.

Node	Case 1			Case 2		
	P_x kips (kN)	P_y kips (kN)	P_z kips (kN)	P_x kips (kN)	P_y kips (kN)	P_z kips (kN)
17	5.0(22.5)	5.0(22.5)	-5.0(22.5)	0.0	0.0	-5.0(22.5)
18	0.0	0.0	0.0	0.0	0.0	-5.0(22.5)
19	0.0	0.0	0.0	0.0	0.0	-5.0(22.5)
20	0.0	0.0	0.0	0.0	0.0	-5.0(22.5)

Table 5: Optimal design comparison for the seventy two-bar spatial truss.

Element group		Optimal cross-sectional areas (in^2)							
		Erbatur et al. [32]	Camp & Bichon [33]	Perez & Behdinan [34]	Camp [1]	Kaveh & Talatahari [30]	Kaveh & Khayatazad [35]	Present study	
		GA	ACO	PSO	BB-BC	HBB-BC	RO	(in^2)	(cm^2)
1	A_1-A_4	1.755	1.948	1.7427	1.8577	1.9042	1.83649	1.85920	11.99481
2	A_5-A_{12}	0.505	0.508	0.5185	0.5059	0.5162	0.502096	0.49308	3.18115
3	A_{13}-A_{16}	0.105	0.101	0.1000	0.1000	0.1000	0.100007	0.10025	0.64677
4	A_{17}-A_{18}	0.155	0.102	0.1000	0.1000	0.1000	0.10039	0.10178	0.65664
5	A_{19}-A_{22}	1.155	1.303	1.3079	1.2476	1.2582	1.252233	1.28534	8.29250

6	A_{23}-A_{30}	0.585	0.511	0.5193	0.5269	0.5035	0.503347	0.51307	3.31012
7	A_{31}-A_{34}	0.100	0.101	0.1000	0.1000	0.1000	0.100176	0.10073	0.64987
8	A_{35}-A_{36}	0.100	0.100	0.1000	0.1012	0.1000	0.100151	0.10248	0.66116
9	A_{37}-A_{40}	0.460	0.561	0.5142	0.5209	0.5178	0.572989	0.51214	3.30412
10	A_{41}-A_{48}	0.530	0.492	0.5464	0.5172	0.5214	0.549872	0.52547	3.39012
11	A_{49}-A_{52}	0.120	0.100	0.1000	0.1004	0.1000	0.100445	0.10029	0.64703
12	A_{53}-A_{54}	0.165	0.107	0.1095	0.1005	0.1007	0.100102	0.10297	0.66432
13	A_{55}-A_{58}	0.155	0.156	0.1615	0.1565	0.1566	0.157583	0.15597	1.00626
14	A_{59}-A_{66}	0.535	0.550	0.5092	0.5507	0.5421	0.52222	0.55473	3.57890
15	A_{67}-A_{70}	0.480	0.390	0.4967	0.3922	0.4132	0.435582	0.40627	2.62109
16	A_{71}-A_{72}	0.520	0.592	0.5619	0.5922	0.5756	0.597158	0.59617	3.84625
Weight (lb)		385.76	380.24	381.91	379.85	379.66	380.458	380.05819	1690.58306 (N)
Average Weight (lb)		N/A	383.16	N/A	382.08	381.85	382.5538	389.14389	
Number of structural analyses		N/A	18,500	N/A	19,621	13,200	19,084	20,000	

4.3 A 200-bar planar truss considering frequency constraints

This case study is a planar 200-bar truss structure shown in Fig.10. The elastic modulus of the material is $2.1\times10^{11}\,N/m^2$ while mass density is $7860\,kg/m^3$. Only the frequency constraints are included in the optimization process. The structure can be divided into 29 groups of elements as shown in Table 6, as in the previous static constraints (stress and displacement) studies. The lower bound cross-sectional area of all design variables is limited to $0.1\,cm^2$.

First, second and third natural frequencies are lower bounded to be more than 5, 10 and 15 *Hz*, respectively. Lumped masses of 100 *kg* are assigned to the nodes at the top of the structure. Table 7 shows the optimal results obtained by bat algorithm and previous works. As indicated in Table 8, it can be seen that all of the constraints are satisfied.

Optimum designs found by bat algorithm are the best overall. BA has found the optimum design after about 25,000 structural analyses corresponding to 50 bats and 500 iterations due to large search space of the problem. Here, $\theta_{\max}$ and $\theta_{\min}$ are taken as 5 and 0.001, respectively. Fig.11 shows the convergence progress of the average of ten independent optimization runs and the best optimization run.

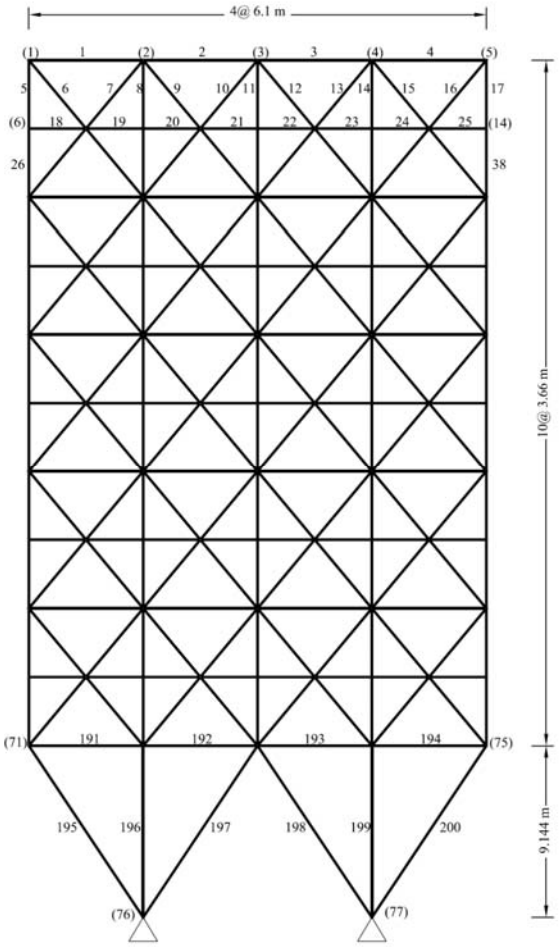

Figure 10. A Planar 200-bar truss.

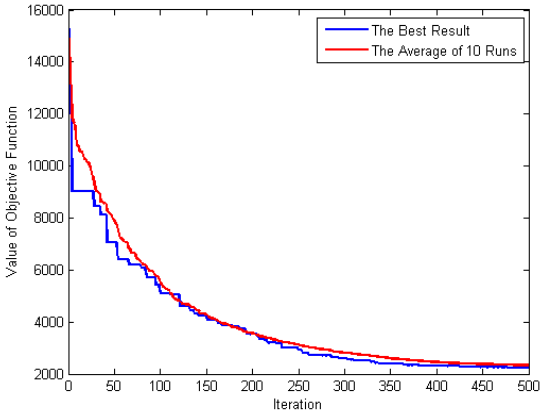

Figure 11. The convergence history for the 200-bar truss obtained by the BA.

Table 6: Member group details for the planar 200-bar truss.

Element group	Member number	Element group	Member number
1	1, 2, 3, 4	16	82, 83, 85, 86, 88, 89, 91, 92, 103, 104, 106, 107, 109, 110, 112, 113
2	5, 8, 11, 14, 17	17	115, 116, 117, 118
3	19, 20, 21, 22, 23, 24	18	119, 122, 125, 128, 131
4	18, 25, 56, 63, 94, 101, 132, 139, 170, 177	19	133, 134, 135, 136, 137, 138
5	26, 29, 32, 35, 38	20	140, 143, 146, 149, 152
6	6, 7, 9, 10, 12, 13, 15, 16, 27, 28, 30, 31, 33, 34, 36, 37	21	120, 121, 123, 124, 126, 127, 129, 130, 141, 142, 144, 145, 147, 148, 150, 151
7	39, 40, 41, 42	22	153, 154, 155, 156
8	43, 46, 49, 52, 55	23	157, 160, 163, 166, 169
9	57, 58, 59, 60, 61, 62	24	171, 172, 173,174, 175, 176
10	64, 67, 70, 73, 76	25	178, 181, 184, 187, 190
11	44, 45, 47, 48, 50, 51, 53, 54, 65, 66, 68, 69, 71, 72, 74, 75	26	158, 159, 161, 162, 164, 165, 167, 168, 179, 180, 182, 183, 185, 186, 188, 189
12	77, 78, 79, 80	27	191, 192, 193, 194
13	81, 84, 87, 90, 93	28	195, 197, 198, 200
14	95, 96, 97, 98, 99, 100	29	196, 199
15	102, 105, 108, 111, 114		

Table 7: Optimal design comparison for the planar 200-bar truss.

Element group	Optimal cross-sectional areas (cm^2)		
	Kaveh & Zolghadr [36]		Present study
	CSS	CSS-BBC	BA
1	1.2439	0.2934	0.40416
2	1.1438	0.5561	0.38121
3	0.3769	0.2952	0.12583
4	0.1494	0.1970	0.10000
5	0.4835	0.8340	0.43709
6	0.8103	0.6455	0.84414
7	0.4364	0.1770	0.11662
8	1.4554	1.4796	1.58675
9	1.0103	0.4497	0.20642
10	2.1382	1.4556	1.85576
11	0.8583	1.2238	1.04687
12	1.2718	0.2739	0.10000
13	3.0807	1.9174	3.06720
14	0.2677	0.1170	0.10000
15	4.2403	3.5535	3.27762
16	2.0098	1.3360	1.50602
17	1.5956	0.6289	0.44824
18	6.2338	4.8335	4.97758
19	2.5793	0.6062	0.15685
20	3.0520	5.4393	3.69226
21	1.8121	1.8435	2.26427
22	1.2986	0.8955	0.62648
23	5.8810	8.1759	7.79338
24	0.2324	0.3209	3.64212
25	7.7536	10.98	6.96567
26	2.6871	2.9489	3.33012
27	12.5094	10.5243	10.96128
28	29.5704	20.4271	19.58939
29	8.2910	19.0983	15.59020
Total mass (kg)	2559.86	2298.61	2234.33397

Table 8: Natural frequencies comparison of optimal design for the 200-bar truss.

Frequency no.	Kaveh & Zolghadr [36],CSS	Kaveh & Zolghadr [36],CSS-BBBC	Present study
1	5.000	5.010	5.0012
2	15.961	12.911	12.9291
3	16.407	15.416	15.0942
4	20.748	17.033	17.0751
5	21.903	21.426	21.0042
6	26.995	21.613	21.9117

4.4 A 72-bar spatial truss considering frequency constraint

A 72-bar space truss is considered for structural design optimization incorporating frequency constraints as shown in Fig.12. This structure topologically is identical to the structure in Example 2, but nodal and element numberings are different. The design variables are the member cross sectional areas, treated as continuous design variables, which are divided into 16 groups in order to maintain the structural symmetry, as shown in Table 9. As can be seen in Fig.12, in the four nodes on the top of the structure (nodes 1–4) it is attached a non-structural mass of 2268 *kg* (5000 *lb*). The material is aluminum, with elastic modulus equal to 68.95 *GPa* (107 *Psi*) and mass density of $2767.99\ \ kg/m^3\ (0.1\ lb/in^3)$. The natural frequency constraints are $f_1 = 4\,Hz$ and $f_3 \geq 6$. The allowable minimum area of the cross sections is $6.45\times10^{-5}\,m^2\ (0.1in^2)$. This problem was also studied by [18] via the so-called Dual Method (DM). [19] utilized the Force Method (FM). Recently, [2], using particle swarm optimization algorithm (PSO), solved this problem. [20] used two of the most recent metaheuristic algorithms: Harmony Search (HS) and Firefly Algorithm (FA), to solve truss sizing optimization with multiple natural frequency constraints. In this article, proposed improved version of bat algorithm is selected and adjusted to overcome this problem. The convergence progress of ten independent runs that is accomplished for this problem is depicted in Fig.13. As it can be observed in Table 10, the result of bat algorithm is better than the results of the literature works and lighter truss structure has been obtained considering multiple frequency constraints. It is important to point out that in this paper, first frequency constraint slightly is violated but it is very small, in other words, it can be neglected as may be seen from Table 11. Here, $\theta_{\max}$ and $\theta_{\min}$ are taken as 1 and 0.001, respectively.

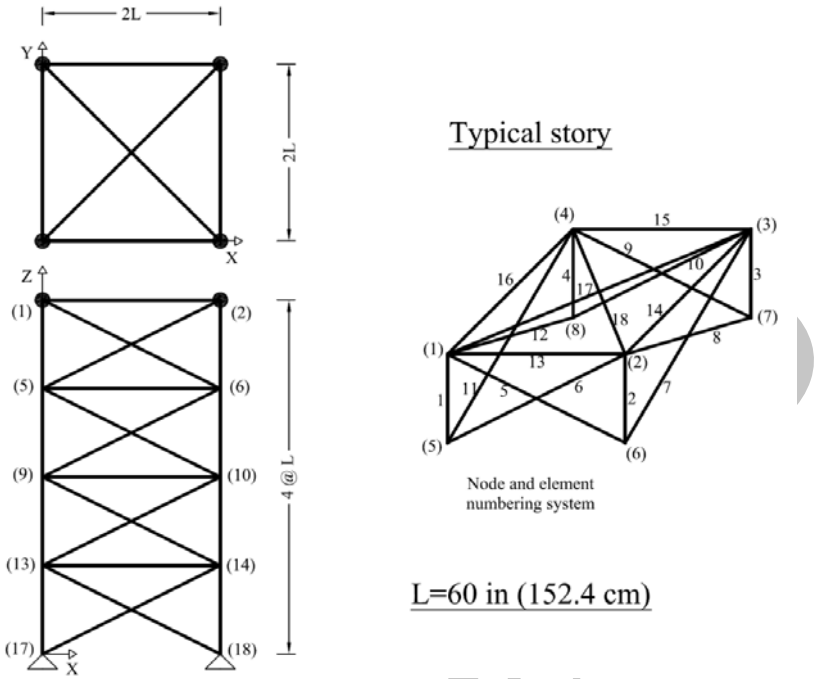

Figure 12. A seventy two-bar truss.

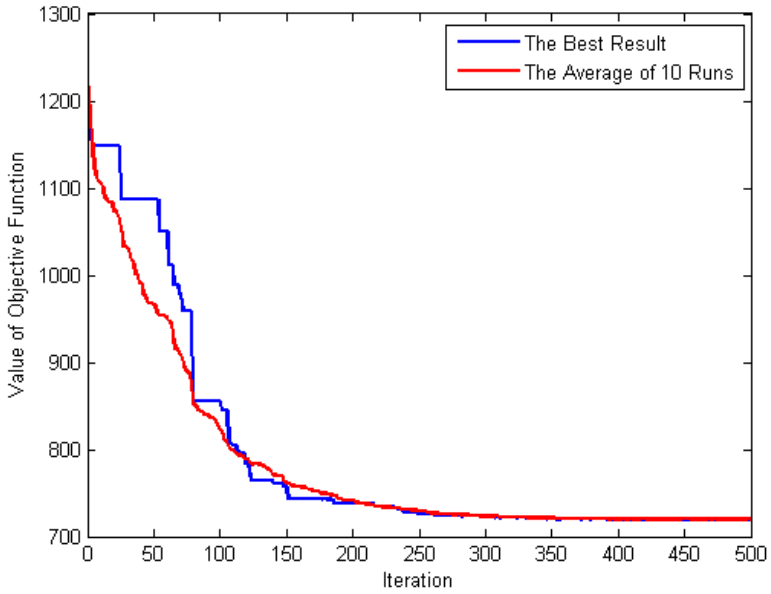

Figure 13. The convergence history for the seventy two-bar spatial truss considering frequency constraint obtained by the BA.

Table 9: Member group details for the 72-bar space truss

Group number	Members
1	1–4
2	5–12
3	13–16
4	17–18
5	19–22
6	23–30
7	31–34
8	35–36
9	37–40
10	41–48
11	49–52
12	53–54
13	55–58
14	59–66
15	67–70
16	71–72

Table 10: Optimal design comparison for the 72 bar space truss with frequency constraints

Element group	Optimal cross-sectional areas (cm^2)								
	Konzelman [18]	Sedaghati [19]	Gomes [2]	Miguel et al. [20],HS	Miguel et al. [20],FA	Kaveh & Zolghadr [36],CSS	Kaveh & Zolghadr [36],CSS-BBBC	Present study	
								(cm^2)	(in^2)
1	3.499	3.499	2.987	3.6803	3.3411	2.528	2.854	3.49980	0.54247
2	7.932	7.932	7.849	7.6808	7.7587	8.704	8.301	8.06315	1.24979
3	0.645	0.645	0.645	0.645	0.645	0.645	0.645	0.64516	0.10000
4	0.645	0.645	0.645	0.645	0.645	0.645	0.645	0.64516	0.10000
5	8.056	8.056	8.765	9.4955	9.0202	8.283	8.202	8.50521	1.31831
6	8.011	8.011	8.153	8.287	8.2567	7.888	7.043	7.90676	1.22555
7	0.645	0.645	0.645	0.645	0.645	0.645	0.645	0.64632	0.10018
8	0.645	0.645	0.645	0.6461	0.645	0.645	0.645	0.65006	0.10076
9	12.812	12.812	13.45	11.451	12.045	14.666	16.328	12.94043	2.00577
10	8.061	8.061	8.073	7.899	8.0401	6.793	8.299	8.00353	1.24055
11	0.645	0.645	0.645	0.6473	0.645	0.645	0.645	0.65471	0.10148
12	0.645	0.645	0.645	0.645	0.645	0.645	0.645	0.64581	0.10010
13	17.279	17.279	16.684	17.406	17.38	16.464	15.048	16.47984	2.55438
14	8.088	8.088	8.159	8.2736	8.0561	8.809	8.268	7.98315	1.23739

Element group	Optimal cross-sectional areas (cm^2)								
	Konzelman [18]	Sedaghati [19]	Gomes [2]	Miguel et al. [20],HS	Miguel et al. [20],FA	Kaveh & Zolghadr [36],CSS	Kaveh & Zolghadr [36],CSS-BBBC	Present study	
								(cm^2)	(in^2)
15	0.645	0.645	0.645	0.645	0.645	0.645	0.645	0.64516	0.10000
16	0.645	0.645	0.645	0.645	0.645	0.645	0.645	0.64516	0.10000
Total Mass (kg)	327.605	327.605	328.823	328.334	327.691	328.814	327.507	326.00504	718.71810 (lb)

Table 11: Natural frequencies comparison of optimal design for the 72 bar space truss.

Frequency no.	Konzelman [18]	Sedaghati [19]	Gomes [2]	Miguel et al. [20, 31] ,HS	Miguel et al. [20],FA	Kaveh & Zolghadr [36],CSS	Kaveh & Zolghadr [36],CSS-BBBC	Present study
1	4.0000	4.0000	4.0000	4.0000	4.0000	4.000	4.000	3.9999
2	4.0000	4.0000	4.0000	4.0000	4.0000	4.000	4.000	3.9999
3	6.0000	6.0000	6.0000	6.0000	6.0000	6.006	6.004	5.9998
4	6.2470	6.2470	6.2190	6.2723	6.2468	6.210	6.2491	6.2686
5	9.0740	9.0740	8.9760	9.0749	9.0380	8.684	8.9726	9.1031

4.5 Eight-story frame under static loading

This 8-story frame structure has been optimized by [21, 22] using the optimality criterion method. [23] optimized it via genetic algorithm. Optimum design procedure using ant colony optimization is performed by [24].

The 24 members of the structure have been categorized into eight groups, as indicated in Fig.14. The lateral displacement at the top of the structure is the only performance constraint (limited to 2 *in*). The modulus of elasticity is taken as E =200 *GPa (*29×10^3 *ksi*) and for the material density $\rho = 76.8\ kN/m^3$ $(2.83\times10^{-4}\ kips/in^3)$. A set of 273 discrete W-sections from American Institute of Steel Construction (AISC) shapes database v14.0 are used for the possible cross-sectional areas of each member. Fig.15 shows the history of optimization for iterations. By proposed improvement for bat algorithm, it can be simply used for discrete optimization problems, θ_{max} and θ_{min} are taken as 14 and 0.1, respectively. In Table 12 the results of designs performed by the present algorithm are depicted. Top displacement of the attained optimum structure is equal to 1.9868769 inch, so the constraint is not violated. Values of θ for discrete optimization are larger than continuous ones. Because discrete domain space is along with greater design variable intervals.

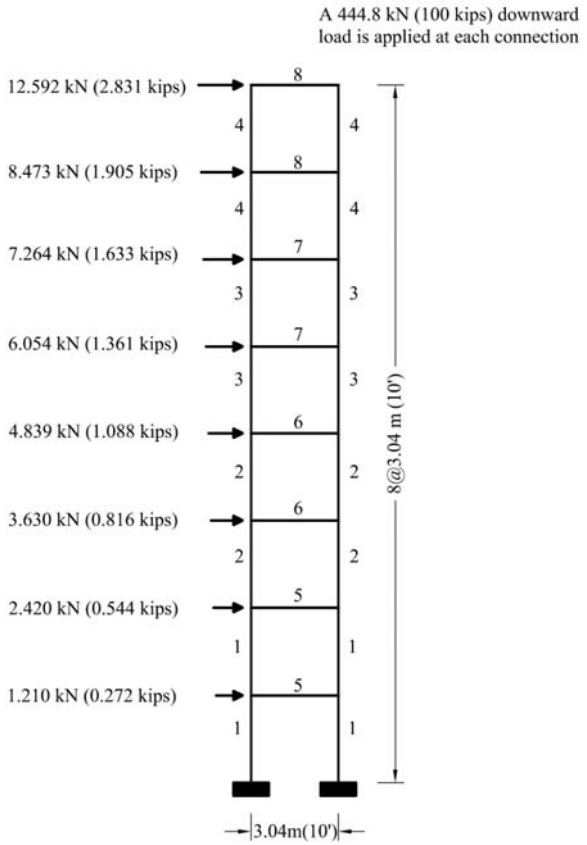

Figure 14. An eight-story planar moment frame under static loading.

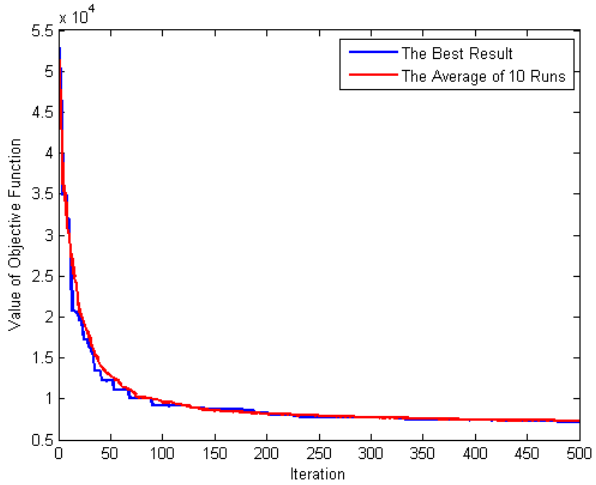

Figure 15. The convergence history for the eight-story moment frame under static loading obtained by the BA.

Table 12: Optimal design comparison for the eight story moment frame under static loading

Group number	Number of members	Narendra S Khot et al. [21]	Camp et al., [23]	Kaveh & Shojaee [24]	Present study
1	4	W14×34	W18×46	W21×50	W18×35
2	4	W10×39	W16×31	W16×26	W16×31
3	4	W10×33	W16×26	W16×26	W16×31
4	4	W8×18	W12×16	W12×14	W12×14
5	2	W21×68	W18×35	W16×26	W18×35
6	2	W24×55	W18×35	W18×40	W18×35
7	2	W21×50	W18×35	W18×35	W18×35
8	2	W12×40	W16×26	W14×22	W16×31
Total weight kN (kips)		41.02(9.22)	32.83(7.38)	31.68(7.12)	31.86492(7.16352)

4.6 Eight-story frame under time history dynamic loading

An eight-story frame structure subjected to time history dynamic loading of El Centro (S-N component, 1940, PGA=0.349g) earthquake record with 2688 points and time interval of 0.02 second is performed. This example is an extremely nonlinear optimization problem that is recently solved by [14] via charged system search (CSS) and an improved harmony search (IHS) algorithms. The 16 design variables for the 8-story moment frame consist of 8 groups for columns and 8 groups for beams as shown in Fig.16.

In order to achieve an optimal weight for this frame, an appropriate algorithm should be used with well-tuned parameters, because the frame has 90 DOFs and the dynamic analysis process is very time consuming. Here, bat algorithm is chosen as an optimizer. Four optimization runs is performed for this design and convergence curves are shown in Fig.17. The linear (elastic) time history dynamic structural analysis is performed using the Newmark-Beta direct integration method.

Drift constraints are as follows:

$$\frac{\delta_i - \delta_{i-1}}{h_i} < DR_a \quad i = 1,2,...,ns \tag{14}$$

Where δ_i is the lateral displacement of the center of the mass in the story i, h_i is the height of the story i, and DR_a is the allowable drift ratio of each story. ns is the number of the frame stories. This constraint is time-dependent.

Dynamic equilibrium equation of a structure under seismic loading can be expressed as:

$$M\ddot{u}(t) + C\dot{u}(t) + K u(t) = -Mr\ddot{u}_g(t) \tag{15}$$

$$r = \begin{cases} r_k = 1 & \text{for x direction DOFs} \\ r_k = 0 & \text{for remaining DOFs} \end{cases} \tag{16}$$

where *M, C,* and *K* are the mass matrix, damping matrix, and stiffness matrix of the structure, respectively. $\ddot{u}(t)$, $\dot{u}(t)$, $u(t)$ are the acceleration, velocity and displacement vectors. The column matrix *r* is an influence coefficient vector which represents the displacements resulting from a unit support displacement. r_k is the *k*th array of the *r* vector. $\ddot{u}_g(t)$ is the ground acceleration scalar value at the time *t*. For damping matrix, the Rayleigh relationship is employed in the analysis.

The drift constraint is imposed to the structure, for more information one can see [14]. The damping ratio is considered as 5 percent. Nodal masses are provided in Table 7**.** It should be noted that only these lumped masses are applied on the frame for dynamic analysis and mass matrix of the frame members is neglected such as prescribed reference. The database of the profiles for discrete optimization is provided in Table 14. The drift constraint is limited to 0.0045, based on the ASCE specification. Objective function is the total weight of frame, where only the weight of the frame members are considered. Weight density and modulus of elasticity are equal to $0.077\ N/cm^3$ and $20593965\ N/cm^3$, respectively. Results of the bat algorithm for this problem are provided in Table 15. Also, comparison of the maximum drift ratios of the optimized 8-story frame designs with their allowable drift ratio is provided in Table 16 showing the constraint is not violated. For this example, $\theta_{\max}$ and $\theta_{\min}$ are selected as 14 and 0.1, respectively.

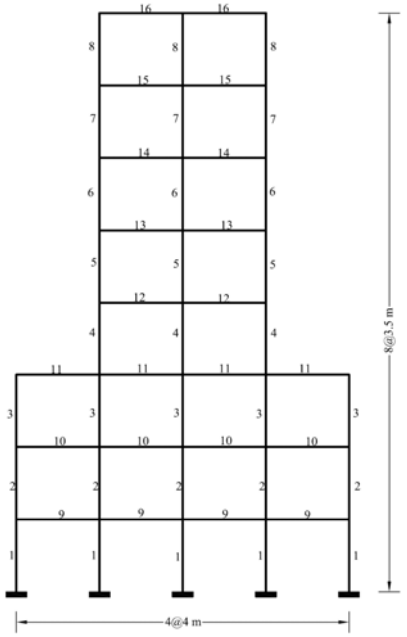

Figure 16. An eight-story planar moment frame under dynamic loading.

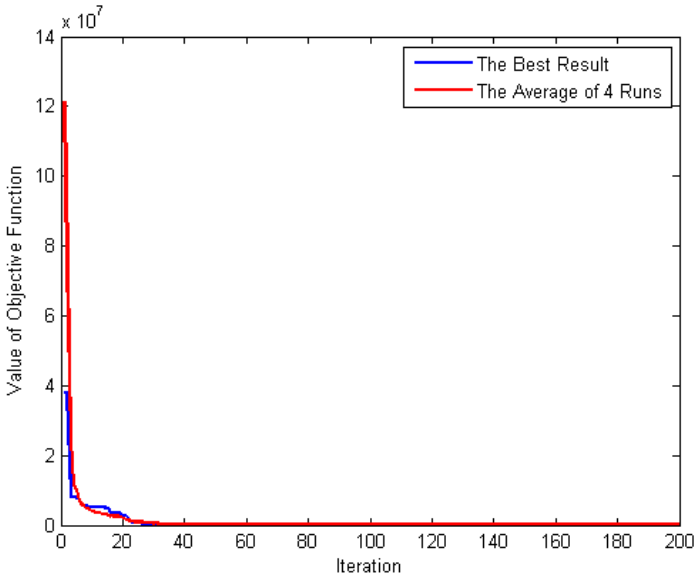

Figure 17. The convergence history for the eight-story moment frame under dynamic loading obtained by the BA.

Table 13: Lumped masses assigned with each node

Inner nodes			**Outer nodes**		
m_{in}			**m_{out}**		
m_x	m_y	m_{θ}	m_x	m_y	m_{θ}
12200 kg	12200 kg	17300 kg.m^2	6100 kg	6100 kg	2500 kg.m^2

Table 14: Available cross-section properties

No	Profile	Area (cm^2)	Moment of Inertia (cm^4)	No	Profile	Area (cm^2)	Moment of Inertia (cm^4)
1	IPE240	39.1	3890	**11**	IPB300	149	25170
2	IPE270	45.9	5790	**12**	IPB320	161	30820
3	IPE300	53.8	8360	**13**	IPB340	171	33660
4	IPE330	62.6	11770	**14**	IPB360	181	43190
5	IPE360	72.7	16270	**15**	IPB400	198	57680
6	IPB200	78.1	5700	**16**	IPB450	218	79890
7	IPB220	91	8090	**17**	IPB500	239	107200
8	IPB240	106	11260	**18**	IPB550	254	136700
9	IPB260	118	14920	**19**	IPB600	270	171000
10	IPB280	131	19270	**20**	IPB650	286	210600

Table 15: Optimal design comparison for the 8-story planar moment frame under dynamic seismic loading

Element group		Optimal cross-sectional areas (cm^2)		
		Kaveh & Zakian [14]		Present study
No.	Cross-section	IHS	CSS	BA
1	A_1	286	286	270
2	A_2	286	286	270
3	A_3	198	286	239
4	A_4	198	286	239
5	A_5	198	286	218
6	A_6	198	239	218
7	A_7	171	198	218
8	A_8	131	198	149
9	A_9	72.7	53.8	39.1
10	A_{10}	198	286	254
11	A_{11}	286	45.9	171
12	A_{12}	286	286	286
13	A_{13}	286	254	286
14	A_{14}	286	198	218
15	A_{15}	254	286	239
16	A_{16}	239	45.9	161
Weight (N)		342330	326630	319697.07000

Table 16: Comparison of the maximum drift ratios of the optimized 8-story frame designs with their allowable ratios subjected to El Centro earthquake record

Story level drift ratio No.	Moment frame with drift constraint			Allowable drift ratio
	Kaveh & Zakian [14]		Present study	
	IHS	CSS	BA	
Level 1	0.00262	0.00250	0.003449	*0.0045*
Level 2	0.00411	0.00321	0.004366	*0.0045*
Level 3	0.00396	0.00383	0.003806	*0.0045*

Level 4	0.00441	0.00444	0.004485	*0.0045*
Level 5	0.00455	0.00325	0.003979	*0.0045*
Level 6	0.00407	0.00429	0.004028	*0.0045*
Level 7	0.00449	0.00434	0.003776	*0.0045*
Level 8	0.00448	0.00408	0.004420	*0.0045*

4.7 Twelve-story truss tower under time history dynamic loading

The last design example is a truss tower consisting of 314 members and 84 nodes, where all members are categorized into 45 groups employing the symmetry of the structure, illustrated in Figure 18. The material and cross-sectional properties are as follows: the modulus of elasticity and the yield stress of the steel are taken as 10000 *ksi* (68943 *MPa*) and 35 *ksi* (241.3 *MPa*), respectively. The material density is 0.3 lb/in^3 (8304 kg/m^3). It should be noticed that in the Ref. [25], the range of cross-sectional areas varies from 0.5 to 15 in^2 which makes the search space, but here for sake of reducing computational effort, the upper bound of search space is reduced to 12 in^2, therefore, in this study the range of cross-sectional areas is defined from 0.5 to 12 in^2. The nodal displacements are limited to 8 *in* (20.32 *cm*). The radius of gyration of each member (r_i) is expressed in terms of its cross-sectional area as $r_i = aA_i^b$, where a and b are the constants depending on the types of sections selected for the members. In this example, pipe sections of a = 0.799 and b = 0.669 are utilized.

This structure is subjected to the Coalinga ground motion with peak ground acceleration of *2.0g* in both the *x*- and *y*-directions, depicted in Figure 19**.** Hence, here, the influence vector is defined as:

$$r = \begin{cases} r_k = 1 & \text{for x and y directions DOFs} \\ r_k = 0 & \text{for remaining DOFs} \end{cases} \tag{16}$$

Total duration of the selected record is 21.235 seconds, with time interval of 0.005 second leading to 4320 time points. The effective duration of this record finalizes at second 9.51, which leads to 1902 points, thus, dynamic analysis of the structure is accomplished till this time step based on Ref [25].

This example has been solved more than 10 times for parameter tuning and only the average convergence history of four runs with identical parameter values is shown in Figure 20. This figure presents the convergence history of the best solution as well.

According to (AISC 1995), the stress restriction for tension members is $\sigma_{allowable} = 0.6F_y$, in which F_y is the yield stress of steel. For compression members this restriction is given by

$$\sigma_{allowable}=\begin{cases}\left[\left(1-\dfrac{\lambda_i^2}{2C_c}\right)F_y\right]\Big/\left(\dfrac{5}{3}+\dfrac{3\lambda_i}{8C_c}-\dfrac{\lambda_i^3}{8C_c^3}\right) & for \quad \lambda_i<C_c \\ \dfrac{12\pi^2E}{23\lambda_i^2} & for \quad \lambda_i\geq C_c\end{cases} \tag{17}$$

E is the modules of elasticity, $\lambda_i = kl_i/r_i$, the slenderness ratio of member i where k and r_i are the effective length factor and the radius of gyration, respectively, $C_c=\sqrt{2\pi^2E/F_y}$ is the slenderness ratio dividing the elastic and inelastic buckling regions.

This structure before being exposed to ground motions has to sustain the static loads applied on them including their own self-weight. It means to achieve the ultimate response of a structure, the member stresses and nodal displacements calculated by static analysis must sum up to those of calculated by dynamic analysis. For further details about imposing total stress constraint, one can refer to [14].

The best found solution is mentioned in Table 17. Figure 21 and Figure 22 figure out absolute values of the obtained stress ratios and displacement values, respectively. For this example, $\theta_{\max}$ and $\theta_{\min}$ are selected as 1 and 0.001, respectively. 35 bats are selected and the number of iterations is taken as 200. So the number of the objective function evaluations is equal to 7000. Optimum solution is not better than result of the aforementioned reference which was performed without meta-model, but it is better than another case (with incorporating meta-model). Further parameter tuning or increasing the number of iterations shall be lead to better solutions.

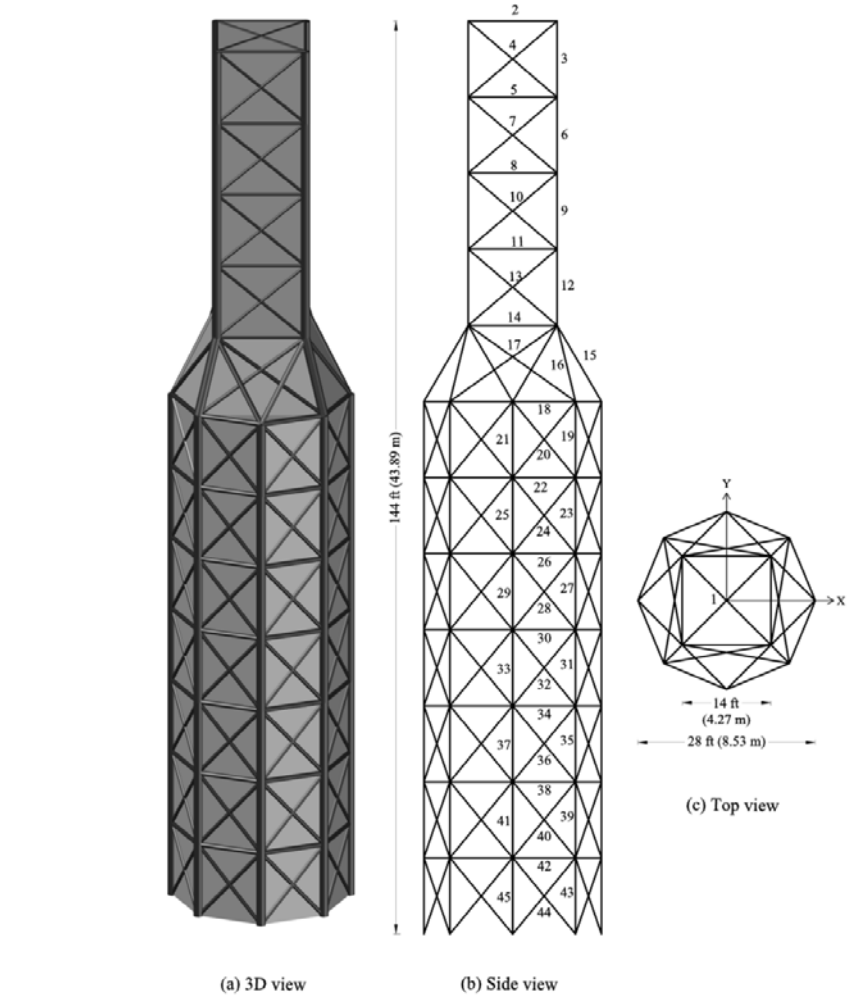

Figure 18. A twelve story truss tower: geometry and member grouping [25].

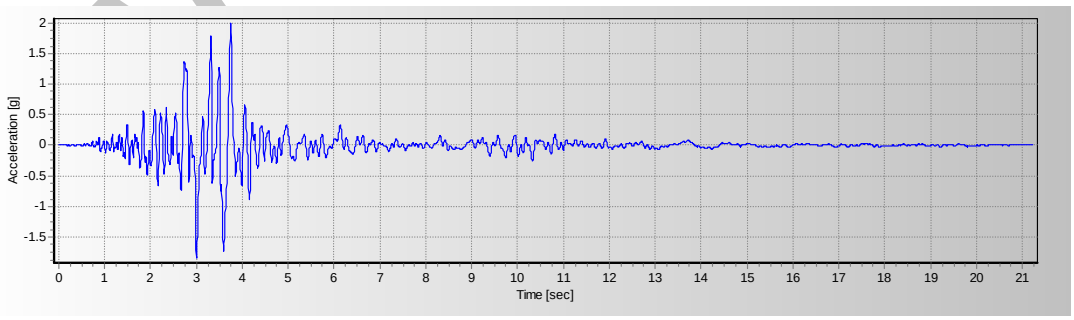

Figure 19. Scaled earthquake record of Coalinga-05 (station: Oil city, 1983, PGA = 2.0 g).

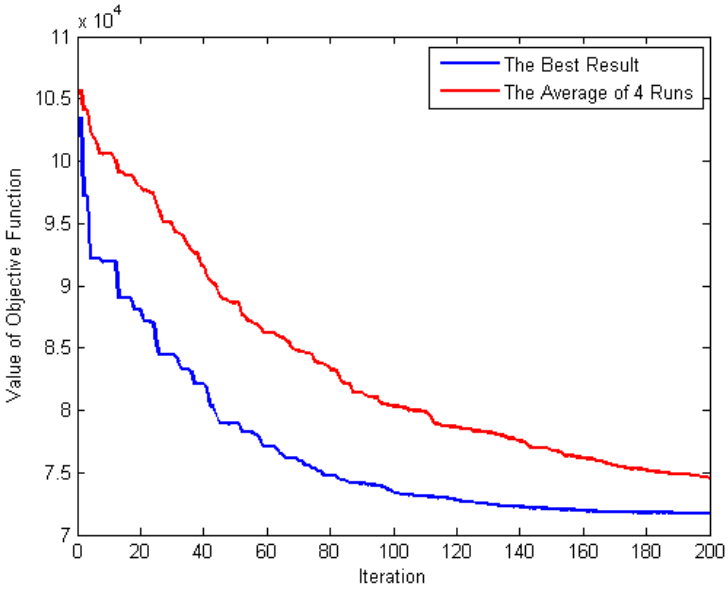

Figure 20. The convergence history for the twelve-story truss tower under dynamic loading obtained by the BA.

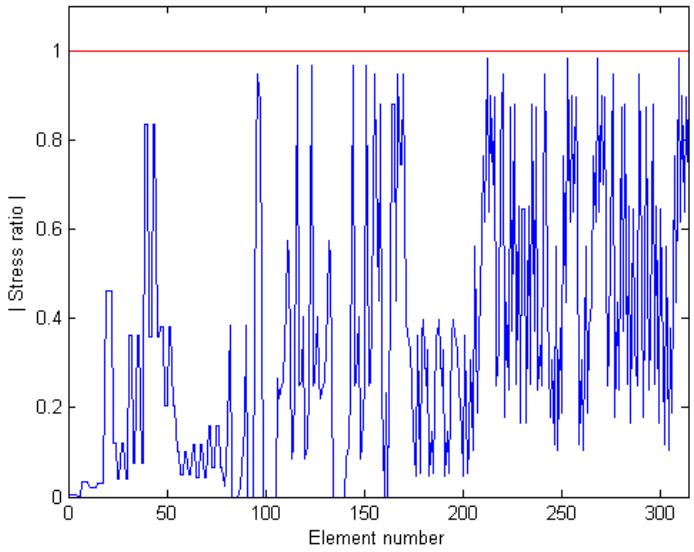

Figure 21. Stress ratios of optimum solution for the truss tower.

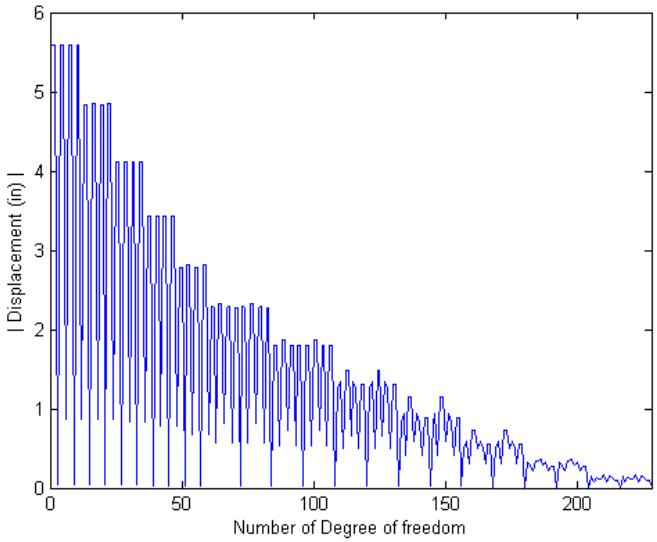

Figure 22. Nodal displacements of optimum solution for the truss tower.

Table 17: Optimal design comparison for the twelve-story truss tower under dynamic seismic loading

Kaveh et al [25]									
Optimal cross-sectional areas (in^2)									
Group No.	Area	Group No.	Area	Group No.	Area	Group No.	Area	Group No.	Area
1	2.0912	10	3.3100	19	6.3445	28	3.66600	37	5.24849
2	1.2039	11	2.2384	20	3.3805	29	6.32790	38	2.6631
3	8.9772	12	5.1180	21	5.3277	30	4.92120	39	11.1094
4	3.2545	13	4.4017	22	2.2399	31	6.77040	40	4.03505
5	8.3155	14	6.8504	23	6.4469	32	3.39510	41	5.27015
6	6.0712	15	6.1707	24	3.6142	33	11.70200	42	3.22022
7	2.8874	16	9.1762	25	3.4791	34	2.37664	43	7.61367
8	4.754	17	1.7435	26	2.2465	35	7.77521	44	4.4382
9	6.8169	18	8.8065	27	7.0078	36	3.83677	45	7.29304
Weight = 68783 lb (31199 kg) without meta-model						Number of structural analysis = 8352			
Weight = 72006 lb (32661 kg) with meta-model						Number of structural analysis = 8591			
Present study									
Optimal cross-sectional areas (in^2)									
Group No.	Area	Group No.	Area	Group No.	Area	Group No.	Area	Group No.	Area
1	7.27991	10	6.62126	19	4.92187	28	4.10477	37	5.87967
2	9.17897	11	11.26577	20	3.96622	29	3.84340	38	6.89639
3	5.80939	12	3.81637	21	5.95883	30	2.91791	39	3.88387
4	2.75550	13	5.59757	22	2.13438	31	7.78403	40	3.79460
5	2.80413	14	2.04268	23	8.01173	32	3.28494	41	6.15935

6	7.58819	15	3.01986	24	2.54369	33	3.42851	42	7.63224
7	3.56051	16	6.88387	25	7.74382	34	6.03642	43	3.91622
8	5.59871	17	1.34087	26	1.66557	35	5.08316	44	4.46628
9	5.91082	18	6.11623	27	7.09057	36	3.18900	45	3.76706
Weight = 71706.45828 lb (32525.50235 kg)						Number of structural analysis =7000			

5. CONCLUDING REMARKS

In this paper, an improved version of recently proposed natural inspired meta-heuristic bat algorithm is implemented to solve skeletal structures optimization problems. The comparisons of numerical results of various structural design optimizations using the BA method with the results obtained by other meta-heuristic and evolutionary approaches are performed to demonstrate the robustness of the present algorithm.

Different types of optimization problems lead to reliable assessment of the algorithm. Also, proposed improvement can simply adjust the algorithm for discrete optimization problems. This algorithm has appropriate exploration ability and can be used for various discrete or continuous optimization problems.

REFERENCES

1. Camp C. Design of space trusses using Big Bang–Big Crunch optimization, *Journal of Structural Engineering*, **133**(2007) 999-1008.
2. Gomes HM. Truss optimization with dynamic constraints using a particle swarm algorithm, *Expert Systems with Applications*, **38**(2011) 957-68.
3. Li LJ, Huang ZB, Liu F, Wu QH. A heuristic particle swarm optimizer for optimization of pin connected structures, *Computers & Structures*, **85**(2007) 340-9.
4. Prendes Gero MB, García AB, Del Coz Díaz JJ. Design optimization of 3D steel structures: Genetic algorithms vs. classical techniques, *Journal of Constructional Steel Research*, **62**(2006) 1303-9.
5. Salajegheh E, Heidari A. Optimum design of structures against earthquake by adaptive genetic algorithm using wavelet networks, *Structural and Multidisciplinary Optimization*, **28**(2004) 277-85.
6. Liu M, Burns SA, Wen YK. Optimal seismic design of steel frame buildings based on life cycle cost considerations, *Earthquake Engineering & Structural Dynamics*, **32**(2003) 1313-32.
7. Kaveh A, Talatahari S. An improved ant colony optimization for the design of planar steel frames, *Engineering Structures*, **32**(2010) 864-73.
8. Kaveh A, Talatahari S. A novel heuristic optimization method: charged system search, *Acta Mechanica*, **213**(2010) 267-89.
9. Kaveh A, Talatahari S. Optimal design of skeletal structures via the charged system search algorithm, *Structural and Multidisciplinary Optimization*, **41**(2010) 893-911.

10. Kaveh A, Farhoudi N. A new optimization method: Dolphin echolocation, *Advances in Engineering Software*, **59**(2013) 53-70.
11. Kaveh A, Khayatazad M. A new meta-heuristic method: Ray optimization, *Computers & Structures*, **112–113**(2012) 283-94.
12. Gholizadeh S, Salajegheh E. Optimal design of structures subjected to time history loading by swarm intelligence and an advanced metamodel, *Computer Methods in Applied Mechanics and Engineering*, **198**(2009) 2936-49.
13. Kaveh A, Zakian P. Performance based optimal seismic design of RC shear walls incorporating soil-structure interaction using CSS algorithm, *International Journal of Optimization in Civil Engineering*, **2**(2012) 383-405.
14. Kaveh A, Zakian P. Optimal design of steel frames under seismic loading using two meta-heuristic algorithms, *Journal of Constructional Steel Research*, **82**(2013) 111-30.
15. Yang X-S. A new metaheuristic bat-inspired algorithm, in: J. González, D. Pelta, C. Cruz, G. Terrazas, N. Krasnogor (Eds.) *Nature Inspired Cooperative Strategies for Optimization* (NICSO 2010), Springer Berlin Heidelberg, 2010, pp. 65-74.
16. Gandomi A, Yang X-S, Alavi A, Talatahari S. Bat algorithm for constrained optimization tasks, *Neural Computing and Applications*, **22**(2013) 1239-55.
17. Mahdavi M, Fesanghary M, Damangir E. An improved harmony search algorithm for solving optimization problems, *Applied Mathematics and Computation*, **188**(2007) 1567-79.
18. Konzelman CJ. *Dual Methods and Approximation Concepts for Structural Optimization, In: Department Of Mechanical Engineering*, University of Toronto, Department of Mechanical Engineering, 1986.
19. Sedaghati R. Benchmark case studies in structural design optimization using the force method, *International Journal of Solids and Structures*, **42**(2005) 5848-71.
20. Miguel LFF, Fadel Miguel LF. Shape and size optimization of truss structures considering dynamic constraints through modern metaheuristic algorithms, *Expert Systems with Applications*, **39**(2012) 9458-67.
21. Khot NS, Venkayya VB, Berke L. Optimization of Structures for Strength and Stability Requirements, in, DTIC Document, 1973.
22. Khot NS, Venkayya VB, Berke L. Optimum structural design with stability constraints, *International Journal for Numerical Methods in Engineering*, **10**(1976) 1097-1114.
23. Camp C, Pezeshk S, Cao G. Optimized design of two-dimensional structures using a genetic algorithm, *Journal of Structural Engineering*, **124**(1998) 551-9.
24. Kaveh A, Shojaee S. Optimal design of skeletal structures using ant colony optimization, *International Journal for Numerical Methods in Engineering*, **70**(2007) 563-81.
25. Kaveh A, Fahimi-Farzam M, Kalateh-Ahani M. Time-history analysis based optimal design of space trusses: The CMA evolution strategy approach using GRNN and WA, *Structural Engineering and Mechanics*, **44**(2012) 379-403.
26. Lee KS, Geem ZM. A new structural optimization method based on the harmony search algorithm, *Computers & Structures*, **82**(2004) 781-98.
27. Lamberti L. An efficient simulated annealing algorithm for design optimization of truss structures, *Computers & Structures*, **86**(2008) 1936-53.

28. Lamberti L, Pappalettere C. An improved harmony-search algorithm for truss structure optimization, in: Proceedings of the twelfth international conference civil, structural and environmental engineering computing, Civil-Comp Press, Stirlingshire, Scotland, 2009.
29. Kaveh A, Talatahari S. Particle swarm optimizer, ant colony strategy and harmony search scheme hybridized for optimization of truss structures, *Computers & Structures*, **87**(2009) 267-83.
30. Kaveh A, Talatahari S. Size optimization of space trusses using Big Bang–Big Crunch algorithm, *Computers & Structures*, **87**(2009) 1129-40.
31. Degertekin SO. Improved harmony search algorithms for sizing optimization of truss structures, *Computers & Structures*, **92–93**(2012) 229-41.
32. Erbatur F, Hasançebi O, Tütüncü İ, Kılıç H. Optimal design of planar and space structures with genetic algorithms, *Computers & Structures*, **75**(2000) 209-24.
33. Camp C, Bichon B. Design of space trusses using ant colony optimization, *Journal of Structural Engineering*, **130**(2004) 741-51.
34. Perez RE, Behdinan K. Particle swarm approach for structural design optimization, *Computers & Structures*, **85**(2007) 1579-88.
35. Kaveh A, Khayatazad M. Ray optimization for size and shape optimization of truss structures, *Computers & Structures*, **117**(2013) 82-94.
36. Kaveh A, Zolghadr A. Truss optimization with natural frequency constraints using a hybridized CSS-BBBC algorithm with trap recognition capability, *Computers & Structures*, **102–103**(2012) 14-27.